文章编号: 1000–0615(2016)03–0344–11 DOI: 10.11964/jfc.20151210217

鳜*IRAK*4基因的克隆、组织表达及病毒感染后表达分析

林 强[1,2], 杨 淞[3], 李宁求[1,2*], 方 翔[1], 付小哲[1,2],
刘礼辉[1,2], 郭慧芝[1,2], 李万里[3], 吴淑勤[1,3]

(1. 中国水产科学研究院珠江水产研究所, 农业部渔用药物创制重点实验室,
广东省水产动物免疫技术重点实验室, 广东 广州 510380;
2. 淡水水产健康养殖湖北省协同创新中心, 湖北 武汉 430070
3. 四川农业大学动物科技学院, 四川 成都 611130)

摘要: 为了研究鳜IRAK4生物学特性及其在抗病毒免疫应答中的作用, 根据鳜转录组数据中筛选出的IRAK4 unigene序列设计引物, 利用 SMART-RACE 技术克隆得到CDS全长为1389 bp的cDNA (命名为ScIRAK), 编码462个氨基酸, 含有1个N端死亡结构域和1个保守的中央蛋白激酶结构域。采用荧光定量RT-PCR方法分析了*ScIRAK*4在健康鳜各组织中的表达差异及病毒感染后在脾脏中的表达变化, 结果显示, 健康鳜中*ScIRAK*4在肝脏中表达量最大, 与其他组织差异显著, 而在血液、脑和胃中表达量最低; 传染性脾肾坏死病毒(infectious spleen and kidney necrosis virus, ISKNV)感染鳜后*ScIRAK*4的表达量呈现下调趋势, 24 h脾脏中的表达量达到最低, 为对照组的45%; 而鳜弹状病毒 (siniperca chuatsi rhabdovirus, SCRV)感染鳜后*ScIRAK*4的表达量呈现上调趋势, 12 h脾脏中*ScIRAK*4的表达量达到最高, 为对照组的8.17倍, 表明*ScIRAK*4在抗ISKNV和SCRV的免疫应答中可能发挥不同的作用。本研究为进一步揭示*ScIRAK*4的抗病毒免疫反应机制提供了依据。

关键词: 鳜; *ScIRAK*4; 基因克隆; 组织表达
中图分类号: Q 785; S 941 **文献标志码:** A

机体通过模式识别受体(pattern recognition receptors, PRRs)识别相关病原体启动先天性免疫机制抵御病原入侵[1]。Toll样受体 (Toll-like receptors, TLRs)是哺乳动物中经典的PRRs之一, 可以识别病原体病原相关分子模式(pathogen-associated molecular patterns, PAMPs), 激活先天性免疫和获得性免疫[2]。白介素-1受体相关激酶家族(interleukin-1 receptor-associated kinases; IRAKs)参与了TLRs的下游信号通路, 是IL-1受体家族(IL-1, IL-18和IL-33受体)和Toll样受体(TLRs)信号通路中的重要信号分子[3]。IRAK家族共有4个成员: *IRAK*1、*IRAK*2、*IRAKM*和*IRAK*4[4-7]。这些成员有一些相似的结构, 包括保守的N-端死亡结构域、proST结构域和保守的中央激酶结构域[8]。髓样分化因子(myeloid differentiation factor 88, MyD88)通过死亡结构域和IRAKs形成一个Myddosome复合体, 这个复合体包含6个MyD88, 4个IRAK4和4个IRAK2分子[9]。Myddosome复合体上IRAKs的磷酸化通过结合肿瘤坏死因子受体相关因子6(TNF receptor associated factor 6, TRAF6)从而启动NFκB介导的一系列信号通路[10]。近年来, 人和哺乳动物IRAK4相关报道较多, 一方面, 在 HEK293细胞中, IRAK4在IL-1β介导的信号通路中必不可少, IRAK4活性的降

收稿日期: 2015-12-28 **修回日期:** 2016-02-19
资助项目: 国家科技支撑计划(2012BAD25B02); 国家自然科学基金(31502201); 广东省海洋渔业科技与产业发展专项(A201501B12)
通信作者: 李宁求, E-mail: liningq@126.com

低可抑制IL-1的活性，从而降低NFκB的活性[10]；*IRAK*4 基因缺陷小鼠IL-1β/TLR信号通路被阻断，抑制NFκB激活和炎症因子的产生[11]。另一方面，研究显示在人纤维细胞和内皮细胞中降低IRAK1或IRAK4活性，可通过IL-1β诱导激活NFκB和AP-1，产生IL-8，同时也证明IRAK1或IRAK4的活性非TLR-8信号通路所必需[12-14]。综上所述，哺乳动物IRAK4在免疫反应中起着重要作用。

目前多种鱼类的IRAK4也相继被克隆和鉴定，包括斑马鱼(*Danio rerio*)[15]、半滑舌鳎(*Cynoglossus semilaevis*)[16]、松江鲈(*Trachidermus fasciatus*)[17]、点带石斑鱼(*Epinephelus coioides*)[6]、虹鳟(*Oncorhynchus mykiss*)[18]、条石鲷(*Oplegnathus fasciatus*)[19]和红笛鲷(*Lutjanus sanguineus*)[20]等。研究表明，鱼类*IRAK*4基因在细菌、寄生虫和病毒感染后表达量上调或者下调。斑马鱼、半滑舌鳎和松江鲈受到细菌或脂多糖刺激后，*IRAK*4表达量上调[15-17]；点带石斑鱼感染刺激隐核虫后，*IRAK*4表达量增加[6]；条石鲷感染虹彩病毒(rock bream iridovirus, RBIV)后，*IRAK*4表达量上调[19]。而虹鳟感染杀鲑气单胞菌后，*IRAK*4表达量与对照组无显著差异；同样斑马鱼感染乌鳢弹状病毒(snakehead rhabovirus, SHRV)后，*IRAK*4表达量无显著变化[15]。但ISKNV感染CPB细胞转录组结果显示，病毒感染后*IRAK*4基因表达下调，并抑制NFκB通路的激活[21]。因此，鱼类*IRAK*4在不同病原感染过程中可能发挥不同的作用。

为了研究鳜*IRAK*4在抗ISKNV和SCRV 2种病毒感染中的作用，实验克隆了鳜*IRAK*4 cDNA，分析编码基因序列和蛋白结构特征，并检测了*ScIRAK*4在鳜各组织中表达情况及病毒感染后表达变化情况，为阐明*IRAK*4在抗病毒感染过程中的作用提供依据。

1　材料与方法

1.1　实验材料

鳜购自广东省肇庆市某养殖场，体长13~14 cm，体质量 80~90 g。暂养于2500 L的PVC桶中，共150尾，共2周，水温28 °C，持续充氧。攻毒用ISKNV病毒ISKNV-QY株和SCRV病毒SCRV-QY株均由本实验室从鳜鱼上分离保存。总RNA提取试剂盒RNeasy Mini Kit购自Qiagen公司，胶回收试剂盒Gel Extraction Kit购自OMEGA公司，反转录试剂盒TransScript II One-Step gDNA Removal and cDNA Synthesis SuperMix购自北京全式金生物技术有限公司，SMARTer® RACE cDNA Amplification Kit、pMD -18T vector、荧光定量试剂盒SYBR Premix EX TapTM II (Tli RNaseH plus)均购自宝生物工程(大连)有限公司，大肠杆菌感受态细胞DH5α(*E. coli* DH5a)由本实验室保存，PCR引物由广州艾基生物技术有限公司合成。

1.2　总RNA提取和cDNA第一链合成

取健康鳜的脾脏，按照RNeasy Mini Kit试剂盒说明书提取RNA，用核酸蛋白测定仪(Eppendorf BioPhotometer Plus)测定RNA样品的浓度和纯度，同时用1%琼脂糖凝胶电泳检测其完整性。检测合格的总RNA按照SMARTer®试剂盒说明书合成cDNA第一链。

1.3　鳜*IRAK*4 cDNA克隆

对ISKNV感染CPB细胞后转录本中筛选出IRAK4 EST序列，进行PCR扩增和测序验证，并采用Primer Premier 5.0软件设计3'-RACE和5'-RACE特异性引物(表1)。

以SMARTer®试剂盒反转录合成的3'-和5'-RACE cDNA 第一条链为模板，分别利用RACE特异引物*ScIRAK*4-1F、*ScIRAK*4-2F和通用引物UPM进行第一轮PCR。第一轮PCR扩增反应条件: 94 °C 30 s，72 °C 2 min，5个循环；94 °C 30 s，70 °C 30 s，72 °C 2 min，5个循环；94 °C 30 s，68 °C 30 s，72 °C 2 min，25个循环；16 °C，10 min。接着使用*ScIRAK*4-1R、*ScIRAK*4-2R和通用引物NUP配对，以第一轮扩增产物为模板进行第二轮PCR。第二轮PCR为巢式PCR，为模板为第一轮产物稀释50倍，扩增反应条件: 95 °C 3 min；95 °C 30 s，68 °C 30 s，72 °C 2 min，20个循环；16 °C，10 min。

3'-RACE和5'-RACE扩增产物经1.5%琼脂糖凝胶电泳检测，胶回收试剂盒回收目的片段，与PMD18-T载体连接，转化DH5α感受态细胞，37 °C倒置培养过夜，阳性克隆经菌落PCR鉴定后 (所用引物为M13-F和M13-R)，送广州艾基生物技术有限公司测序。将测序所得片段通过DNAStar分析软件拼接，获得该基因cDNA序列。

表 1 本研究所用的引物

Tab. 1 Primers used in this study

引物名称 primer name	序列(5'-3') sequence(5'-3')	用途 usage
*ScIRAK*4-1F	TCGGCTGGCGGGAGTCCAGACAAT	5'RACE
*ScIRAK*4-1R	ACCAGAGCATCGGCCAAGCGGACAT	
*ScIRAK*4-2F	TGTCCGCTTGGCCGATGCTCTGGT	3'RACE
*ScIRAK*4-2R	GGGAAGTCCTCCACTGTCCTGGCAACA	
1507F	CGCTGAGAGGAGAGATC	qPCR
1507R	CTCCATCAAGAACTGTGGC	
β-actin-F	AGAGGGAAATCGTGCGTG	qPCR
β-actin-R	GAAGGAAGGCTGGAAGAGG	

1.4 *ScIRAK*4基因生物信息学分析

采用DNAstar对基因开放阅读框(open reading frame, ORF)进行预测，通过与其他物种 *IRAK*4核苷酸和氨基酸序列比对，最终确定其ORF。采用ProtParam(http://web.expasy.org/protparam/)软件进行蛋白质理化性质预测，通过SignalP 4.0 Server(http://www.cbs.dtu.dk/services/SignalP/)预测信号肽序列，糖基化位点和磷酸化位点的预测采用NetNGlyc 1.0 Server(http://www.cbs.dtu.dk/services/NetNGlyc/)和NetPhos 2.0 Server (http://www.cbs. dtu.dk/services/NetPhos/)软件；采用SOPMA软件(https://npsa-prabi.ibcp.fr/)对蛋白质的二级结构进行预测。通过BlastP程序在PDB数据库中(protein data bank，蛋白晶体结构数据库)对IRAK4蛋白序列进行检索。*IRAK*4序列比对通过ClustalW进行，在比对的基础上采用Modeller程序进行同源模建。ScIRAK4三级结构模型分析采用分子可视化操作软件VMD完成。应用 Clustalx对*ScIRAK*4基因和其他物种*IRAK*4基因编码氨基酸序列进行多序列比对，用MEGA 4.0中的邻接法(neighbor-joining, NJ) 构建进化树。

1.5 *ScIRAK*4基因组织表达分析

选取3尾健康鳜，分别取其鳃、脑、心脏、肝、脾、头肾、中肾、后肾、肠、肌肉、血液和胃组织，按RNeasy Mini Kit照试剂盒说明书提取RNA。分别用电泳仪和核酸蛋白测定仪测定RNA质量和浓度。采用实时荧光定量PCR技术检测*ScIRAK*4 基因在12个组织中的相对表达量。根据获得的*ScIRAK*4 cDNA设计特异检测引物1507F和1507R，内参引物选用本实验室已经发表的β-actin基因引物(表1)[22]。用TransScript II One is SuperMix进行反转录，合成cDNA第一链。以cDNA第一链为模板，在ABI 7500 (Applied Biosystems) 实时荧光定量PCR仪上进行荧光定量PCR扩增。反应体系和反应程序参照时云朵[23]的方法 。采用$2^{-\Delta\Delta Ct}$法计算样品中*ScIRAK*4基因相对表达量。

1.6 病毒感染对*ScIRAK*4基因表达的影响

根据预实验的结果，选取90尾健康鳜，分为ISKNV注射组、SCRV注射组和对照组，每组30尾鱼，水温保持在28 °C左右，不间断充氧。注射前，将细胞培养的病毒离心过滤，置于冰上备用。ISKNV注射组每尾鳜鱼腹腔注射5×10^7PFU ISKNV；SCRV注射组每尾鳜鱼腹腔注射5×10^7PFU SCRV；对照组腹腔注射0.2 mL 0.65%的生理盐水。人工感染后ISKNV组和对照组分别在0、3、6、12、24、48、72、96 h和168 h取3尾鳜的病毒靶器官——脾脏[24]，SCRV组在0、3、6、12、24、48和72 h取3尾鳜的脾脏，保存于–70 °C，并检测*ScIRAK*4基因相对表达量。

2 结果

2.1 *ScIRAK*4 cDNA克隆和序列分析

拼接后获得*ScIRAK*4 cDNA序列，其开放阅读框为1389 bp，编码462个氨基酸，预测其编码蛋白质分子量为51.69 ku，等电点pI为5.33。该氨基酸序列含有1个N端死亡结构域(9~110aa)、1个保守的中央蛋白激酶结构域(187~444aa)(图1)、

3个N-糖基化位点、16个丝氨酸磷酸化位点、6个苏氨酸磷酸化位点和5个酪氨酸磷酸化位点，未发现N端有信号肽序列。在IRAK-4 蛋白二级结构中，α-螺旋占48.48%，β-转角占9.31%，无规则卷曲占29%，延伸链占13.2%。

ScIRAK4氨基酸序列同源比对发现该序列与

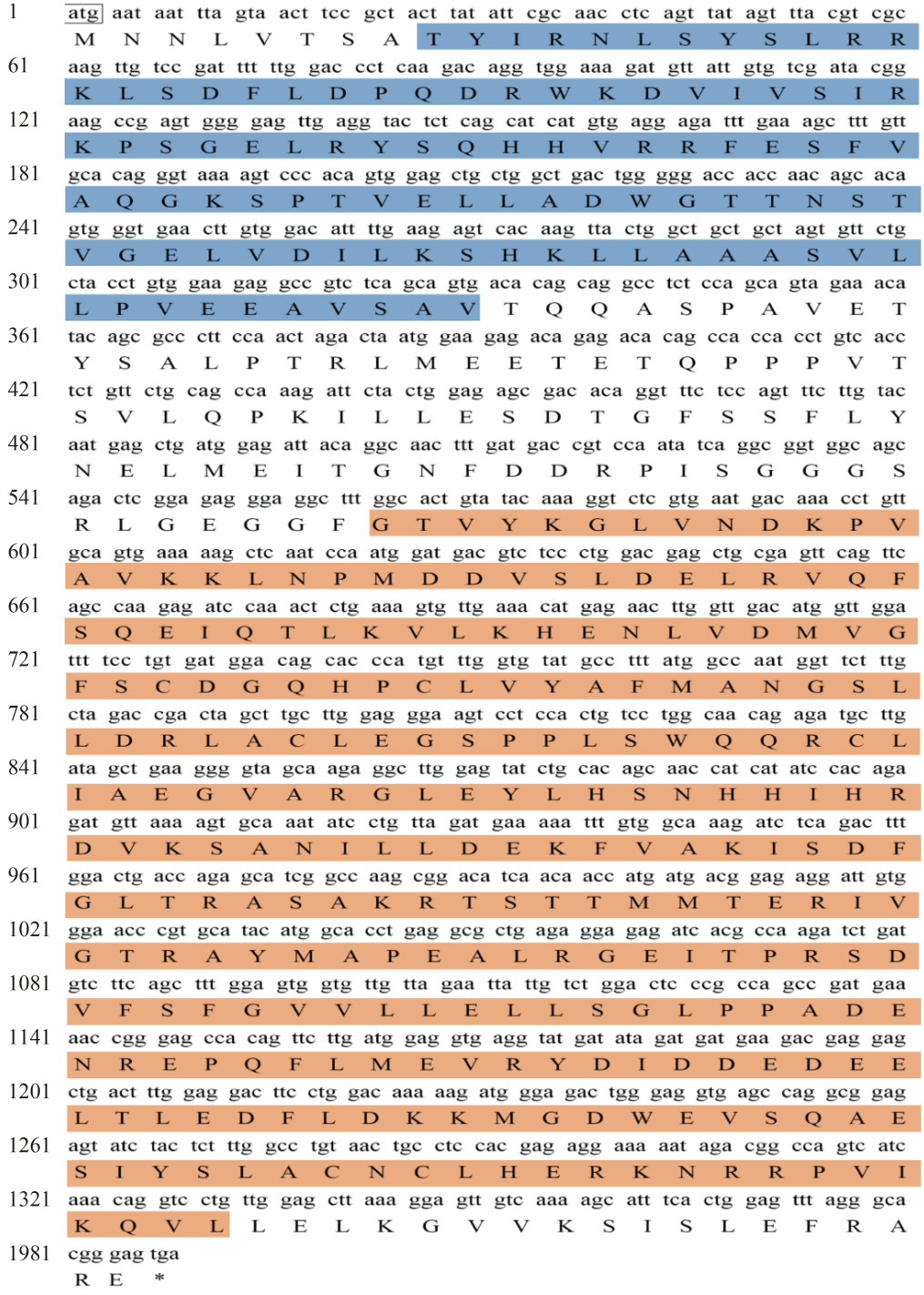

图 1　*ScIRAK4*基因的核苷酸序列及其推导的氨基酸序列

细线方框内的 ATG 为起始密码子； 终止密码子 TGA 由* 标出；death结构域标记为蓝色；Pkinase结构域标记为黄色

Fig. 1　Nucleotide and putative amino acid sequences of *ScIRAK4*

Start codon(ATG) is marked with filament box; asterisk indicates stop codon(TGA); The N-terminal death domain (blue) and C-terminal protein kinases domain (yellow) are shaded

条石鲷的同源性最高，为87%，与红笛鲷和点带石斑鱼的同源性为86%，与松江鲈、大黄鱼(*Larimichthys crocea*)、半滑舌鳎、大西洋鲑(*Salmo salar*)、大西洋鳕(*Gadus morhua*)、虹鳟、香鱼(*Plecoglossus altivelis*)、衰白鲑(*Coregonus maraena*)、斑点叉尾鮰(*Ictalurus punctatus*)的同源性分别为83%、78%、73%、69%、67%、65%、65%、65%、63%，与人(*Homo sapiens*)、原鸡(*Gallus gallus*)、小鼠(*Mus musculus*)和非洲爪蟾(*Xenopus tropicalis*)的同源性均低于60%。氨基酸序列多重比对结果显示，*ScIRAK*4同其他鱼类一样，含有保守的死亡机构域和中央蛋白激酶结构域(图2)。系统进化分析表明，鳜*ScIRAK*4与条石鲷聚在一起，然后与其他鱼类聚在一个大的分支(图3)，1000次自举(Bootstrap)重复检验进化树的置信度。

2.2 ScIRAK4的空间结构预测

从PDB数据库中选取了相似度最高(39%)的人源IRAK4蛋白的晶体结构(PDB编号为2NRU)为模板进行ScIRAK4蛋白的晶体结构预测，共构建了8个初始模型。经过结构优化后，选取了得分最优的模型作为最终的结构模型(图4-a)。IRAK4的结构由10个α螺旋、11段反平行的β转角及数段无规卷曲组成，共含有两个结构域，分别是死亡结构域(9~110aa，图4-b)和中央蛋白激酶结构域(187~444aa，图4-c)。前者由3个α螺旋和2段无规卷曲组成；后者由7个α螺旋、9段反平行的β片层及少量无规卷曲组成，螺旋与转角的位置相对独立，构成2个疏水核心。

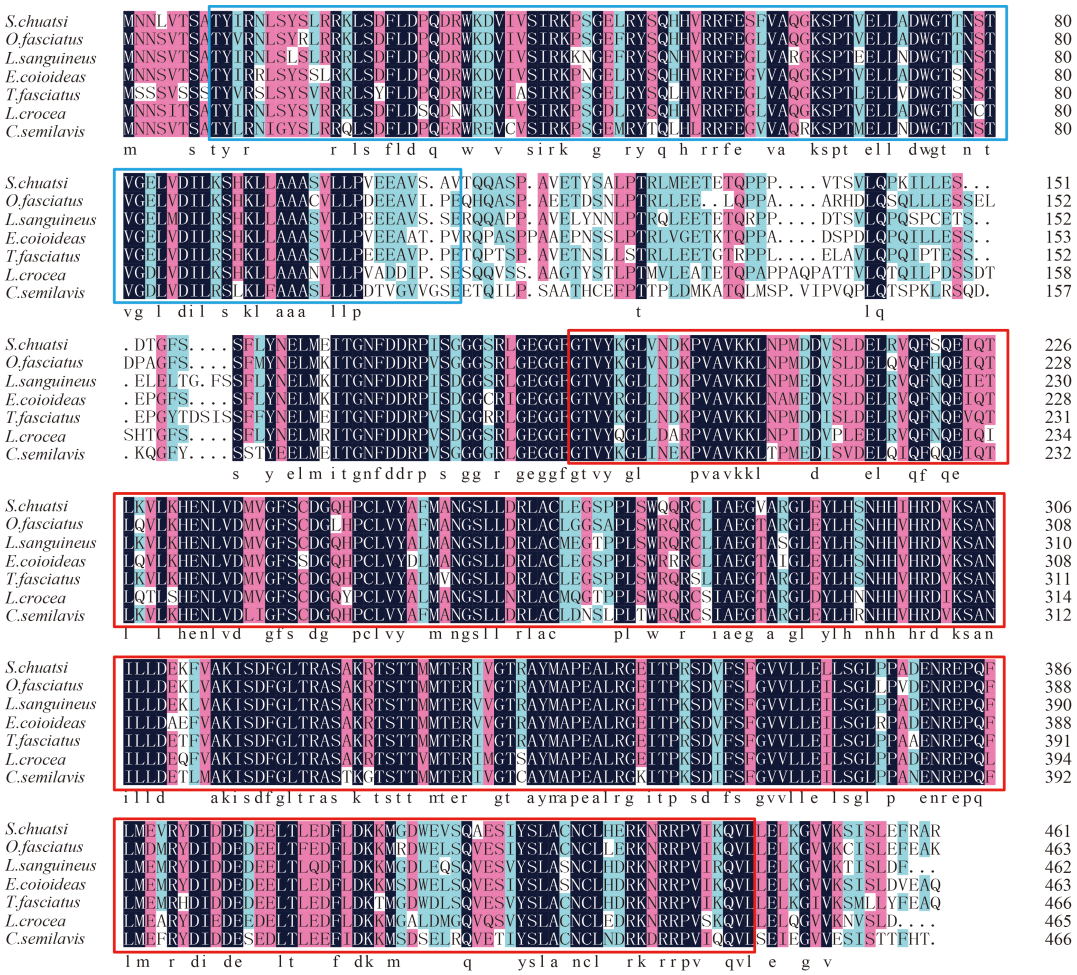

图 2 鳜ScIRAK4氨基酸序列与其他物种IRAK4氨基酸序列比对

蓝色框内代表死亡结构域，红色框内代表蛋白激酶结构域

Fig. 2 Amino acid sequences alignment of ScIRAK4 with other species IRAK4

Amino acid sequences alignment of ScIRAK4 with other species *IRAK4*

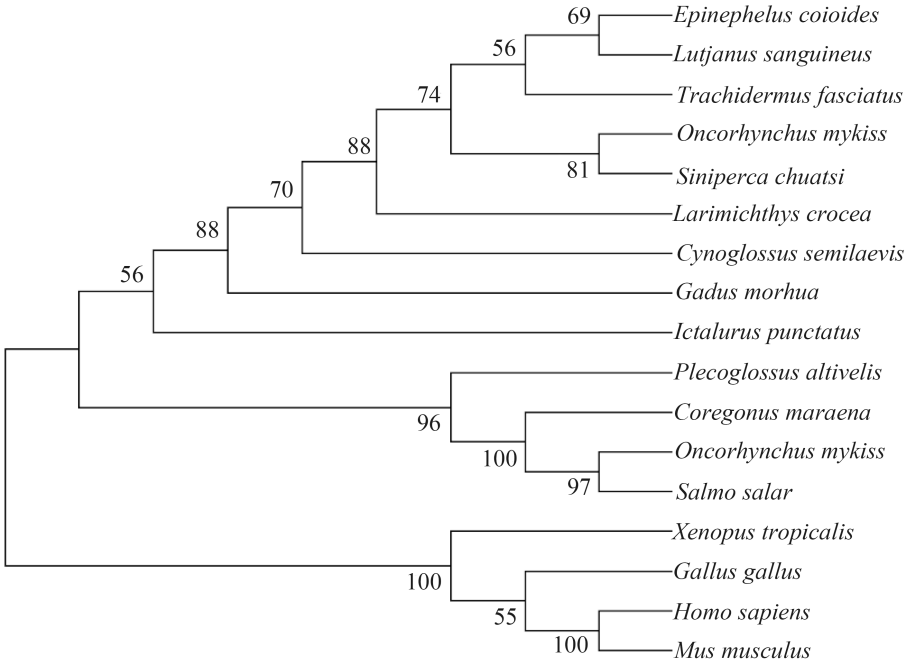

图 3　以NJ法构建的ScIRAK4氨基酸序列及其他物种相关氨基酸序列的进化树

Fig. 3　A phylogenetic tree based on amino acid sequence of ScIRAK4 and related amino acid sequences in other species by the neighbour-joining method

2.3　*ScIRAK4*基因的组织表达分析

*ScIRAK4*基因在所检测12个鳜鱼组织中均有表达(图5)，其中肝脏中的表达量最高，显著高于其他各组织($P<0.05$)；血液、脑和胃中*ScIRAK4*的表达量最低，与其他8个组织中的表达量差异显著($P<0.05$)。肝、肌肉、心脏、鳃、后肾、肠、中肾、头肾、脾脏、胃和脑中*ScIRAK4*的表达量分别是血液中的10.94、4.91、4.06、3.03、2.56、2.19、1.99、1.89、1.79、1.20和1.11倍。

2.4　ISKNV和SCRV感染后*ScIRAK4*表达变化

ISKNV感染后，鳜脾脏中*ScIRAK4*表达量呈现下调趋势，其中3和6 h的表达量与对照组差异不显著，12 h的表达量为对照组的72%，24 h的表达量最低，为对照组的54%($P<0.05$)，48 h~7 d的表达量趋于稳定，为对照组的78%~82%(图6)。

SCRV感染后，鳜脾脏中*ScIRAK4*表达量呈现上调趋势，其中3和6 h的表达量为对照组的2.53和1.90倍，12 h表达量达到最高，为对照组的8.17倍($P<0.01$)，随后表达量开始下降，但均高于对照组，24、48和72 h的表达量分别为对照组的1.99、1.22和1.76倍(图7)。

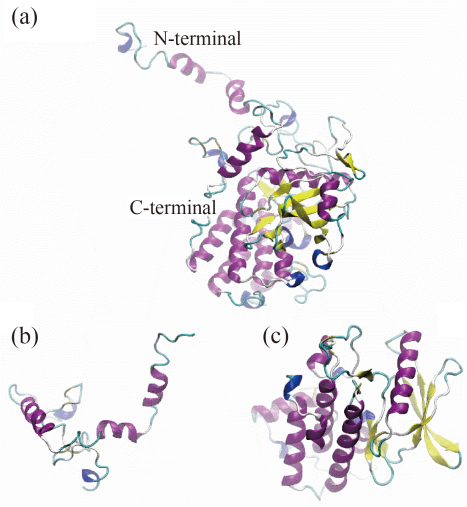

图 4　鳜ScIRAK4的三维结构模拟

(a)鳜ScIRAK4的分子三维结构模型；(b)death区域分子结构图；(c)Pkinase结构域分子结构图

Fig. 4　Predicted three-dimensional structure of ScIRAK4

(a) the predicted three-dimensional structure of ScIRAK4; (b) the predicted structure of death domain; (c) the predicted structure of Pkinase domain

3　讨论

实验获得了鳜*IRAK4* cDNA序列，其开放阅

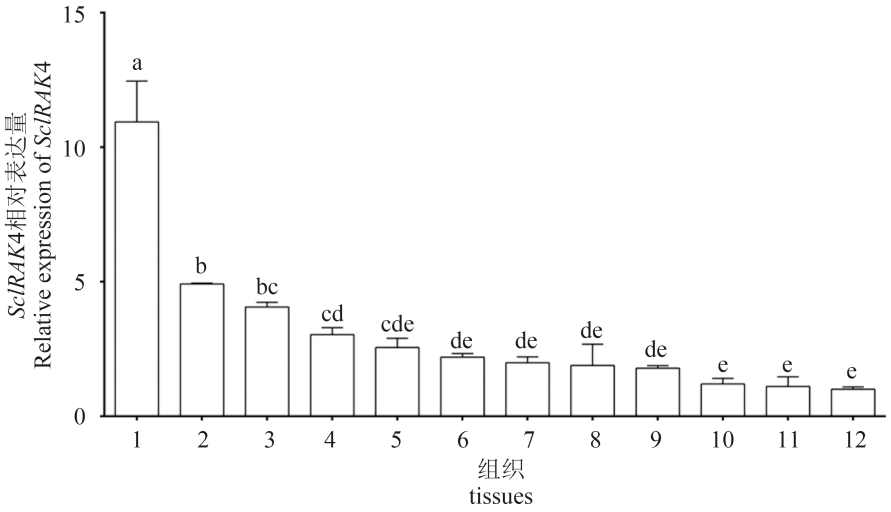

图 5 鳜不同组织中ScIRAK4基因的表达分布

ScIRAK4 mRNA表达量用*β-actin*的表达量进行标准化。数据为3条鱼的平均值。对各组织表达量进行差异显著性分析，用不同的字母表示(P<0.05)。1.肝，2.肌肉，3.心脏，4.鳃，5.后肾，6.肠，7.中肾，8.头肾，9.脾脏，10.胃，11.脑，12.血液

Fig. 5 Tissue distribution of ScIRAK4 mRNA in healthy mandarin fish

The ScIRAK4 mRNA expression levels were normalized to β-actin transcripts, and the data were expressed as means ± standard errors (n=3). Significant differences in the gene's expression between each tissue are indicated with different letters (P<0.05). 1.liver, 2.muscle, 3.heart, 4.gill, 5.hind kidney, 6.intestine, 7.mid kidney, 8.head kidney, 9.spleen, 10.stomach, 11.brain, 12.blood

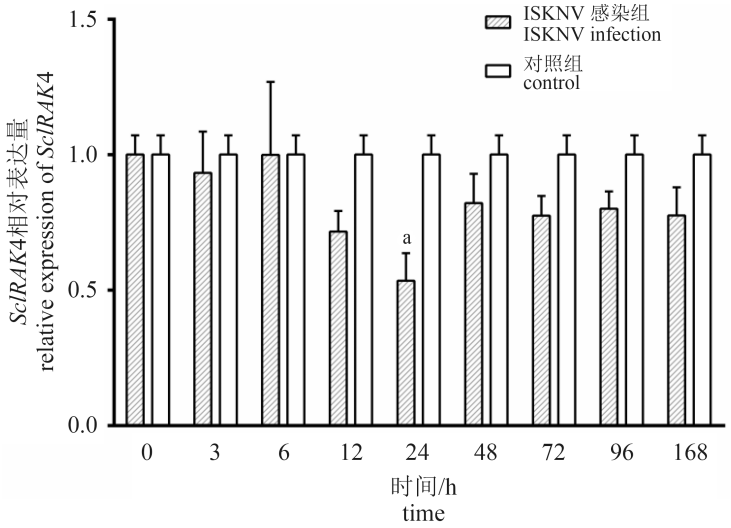

图 6 ISKNV感染后鳜鱼脾脏中*ScIRAK*4表达量的变化

mRNA表达量用0 h的β-actin的表达量进行标准化。数据来自3条鱼的平均值。将不同时间点的ISKNV感染组的*ScIRAK*4表达量与对照组进行显著性差异分析(P<0.05)

Fig. 6 Expression profiles of *ScIRAK*4 in the spleen after infection with ISKNV.

The mRNA expression levels were normalized to the transcripts of β-actin at 0 h. The data were shown as means ± standard errors (n=3). Significant differences in the gene's expression between the control and ISKNV-infected groups at each time point are indicated with letter (P<0.05)

读框为1389 bp，编码462个氨基酸。鳜ScIRAK4与条石鲷的相似度最高，具有死亡结构域和中央激酶结构域，和IRAK家族其他基因相比，ScIRAK4同其他物种的IRAK4一样缺少部分C端区域[25]。在哺乳动物中，MyD88通过与IRAK4死亡结构域中的某些位点结合，激活IRAK4，转导信号给TLRs通路下游的相关因子[26]，在ScIRAK4的死亡结构域中同样发现了MyD88结合位点。这些结果表明，鳜IRAK4的结构和功能与其他鱼类和哺乳动物具有相似性。

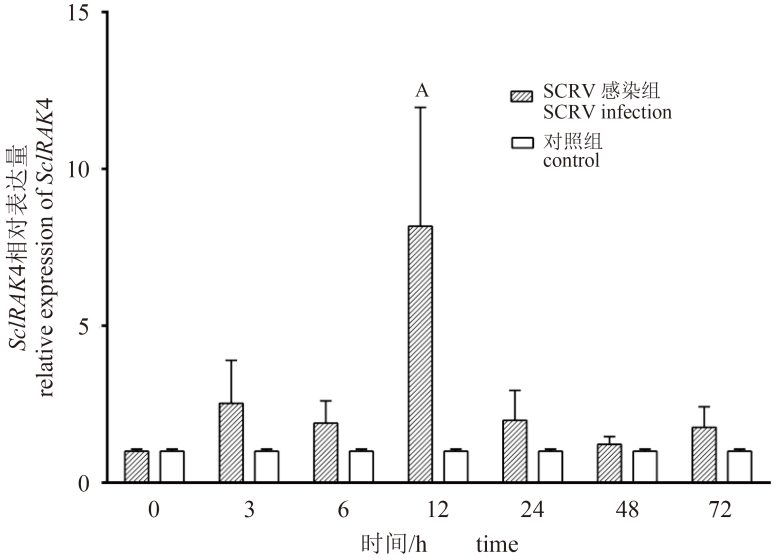

图 7　SCRV感染后鳜鱼脾脏中*ScIRAK*4表达量的变化

mRNA表达量用0 h的β-actin的表达量进行标准化。数据来自3条鱼的平均值。将不同时间点的SCRV感染组的*ScIRAK*4表达量与对照组进行显著性差异分析(P<0.01)

Fig. 7　Expression profiles of *ScIRAK*4 in the spleen after infection with SCRV.

The mRNA expression levels were normalized to the transcripts of *β-actin* at 0 h. The data were shown as means ± standard errors (n=3). Significant differences in the gene's expression between the control and SCRV-infected groups at each time point are indicated with letter (P<0.01)

*ScIRAK*4在肝脏中表达量最大，与其他组织差异显著，其次是肌肉、心脏和鳃，在血液、脑和胃中的表达量最少。哺乳动物中肝脏和肾脏*IRAK*4表达量最高[10]，但在不同鱼类中，*IRAK*4组织表达差异较大[6, 15-20, 27-28]。本研究发现鳜肝脏中*IRAK*4表达量最高与点带石斑鱼[6]、红笛鲷[20]和条石鲷[19]等研究结果一致；而在斑马鱼[15]、半滑舌鳎[16]、虹鳟[18]和香鱼[28]的脾脏和肾脏中*IRAK*4表达量较高，松江鲈[17]的皮肤中*IRAK*4表达量最高。头肾和脾脏是鱼类的主要淋巴器官[29-30]，皮肤是鱼类抵御病原侵入提供免疫保护的第一道防线[31]。而鱼类的肝脏也可能像哺乳动物的肝脏一样富含复杂的免疫相关细胞[32]，例如鱼类的肝脏中含有大量的巨噬细胞和免疫相关的TLR5、IL-6、TNFα、CSFR-1都在肝脏中被检出[33-36]。这可能是*ScIRAK*4在肝脏中的表达量最高的原因之一。

ISKNV感染后24 h，*ScIRAK*4的表达量显著下调，与本实验室前期转录谱分析实验结果一致[21]；而SCRV感染后12 h *ScIRAK*4的表达量显著上调，与已经报道的鱼类IRAK4抗病毒效应不一致。条石鲷感染虹彩病毒(rock bream iridovirus, RBIV)后，*IRAK*4表达上调[19]，而斑马鱼感染乌鳢弹状病毒(snakehead rhabovirus, SHRV)后，*IRAK*4表达量无显著变化[15]。机体通过不同的信号通路识别病原模式受体可能是造成*IRAK*4表达差异的原因。已有研究表明，艾滋病毒、小鼠巨细胞病毒和脑膜炎病毒感染IRAK4功能受损细胞或TLR9功能受损细胞后，干扰素分泌受限制[37-38]。Yang等[39]研究发现，TLR3/4通路产生IFN-α/β/γ不需要IRAK4，TLR7/8和TLR9必须依赖IRAK，但是在人类细胞抗病毒免疫保护中TLR7/8、TLR9通路不是必需的。*ScIRAK*4在ISKNV刺激下表达量下调，并且NF-κB的激活受到抑制，因此，鳜识别和抵御ISKNV的过程可能不是TLR9通路。*ScIRAK*4在SCRV刺激下表达量显著上调，因此鳜识别和抵御SCRV过程中，TLR-7/8-IRAK4-IFN通路可能起着很重要的作用，但是其中的机制还不清楚。进一步研究鳜IRAK1/2/3、MyD88、TLR3、TLR7/8、TLR9在抗病毒免疫应答中的表达变化及与*ScIRAK*4的互作，有助于阐明*ScIRAK*4在鳜抗病毒免疫应答中的作用机制。

参考文献：

[1] Akira S, Uematsu S, Takeuchi O. Pathogen recognition and innate immunity [J]. Cell, 2006, 124(4): 783–801.

[2] Krishnan J, Selvarajoo K, Tsuchiya M, *et al*. Toll-like receptor signal transduction [J]. Experimental and Molecular Medicine, 2007, 39(4): 421–438.

[3] Janssens S, Beyaert R. Functional diversity and regulation of different interleukin-1 receptor-associated kinase (IRAK) family members [J]. Molecular Cell, 2003, 11(2): 293–302.

[4] Cao Z, Henzel W J, Gao X. IRAK: a kinase associated with the interleukin-1 receptor [J]. Science, 1996, 271(5252): 1128–1131.

[5] Wang H, El maadidi S, FIscher J, *et al*. A frequent hypofunctional IRAK2 variant is associated with reduced spontaneous hepatitis C virus clearance [J]. Hepatology, 2015, 62(5): 1375–1387.

[6] Li Y W, Mo X B, Zhou L, *et al*. Identification of IRAK-4 in grouper (*Epinephelus coioides*) that impairs MyD88-dependent NF-κB activation [J]. Developmental and Comparative Immunology, 2014, 45(1): 190–197.

[7] Wesche H, Gao X, Li X, *et al*. IRAK-M is a novel member of the Pelle/interleukin-1 receptor-associated kinase (IRAK) family [J]. Journal of Biological Chemistry, 1999, 274(27): 19403–19410.

[8] Flannery S, Bowie A G. The interleukin-1 receptor-associated kinases: critical regulators of innate immune signalling [J]. Biochemical Pharmacology, 2010, 80(12): 1981–1991.

[9] Lin S C, Lo Y C, Wu H. Helical assembly in the MyD88-IRAK4-IRAK2 complex in TLR/IL-1R signalling [J]. Nature, 2010, 465(7300): 885–890.

[10] Li S, Strelow A, Fontana e J, *et al*. IRAK-4: a novel member of the IRAK family with the properties of an IRAK-kinase [J]. Proceedings of the Ntional Aademy of Siences of The United States of America, 2002, 99(8): 5567–5572.

[11] Kim T W, StaschkE K, Bulek K, *et al*. A critical role for IRAK4 kinase activity in Toll-like receptor-mediated innate immunity [J]. Journal of Experimental Medicine, 2007, 204(5): 1025–1036.

[12] Qin J, Jiang Z, Qian Y, *et al*. IRAK4 kinase activity is redundant for interleukin-1 (IL-1) receptor-associated kinase phosphorylation and IL-1 responsiveness [J]. Journal of Biological Chemistry, 2004, 279(25): 26748–26753.

[13] Qin J, Yao J, Cui G, *et al*. TLR8-mediated NF-kappaB and JNK activation are TAK1-independent and MEKK3-dependent [J]. Journal of Biological Chemistry, 2006, 281(30): 21013–21021.

[14] Song K W, Talamas F X, Suttmann R T, *et al*. The kinase activities of interleukin-1 receptor associated kinase (IRAK)-1 and 4 are redundant in the control of inflammatory cytokine expression in human cells [J]. Molecular Immunology, 2009, 46(7): 1458–1466.

[15] Phelan P E, Mellon M T, Kim C H. Functional characterization of full-length TLR3, IRAK-4, and TRAF6 in zebrafish (*Danio rerio*) [J]. Molecular Immunology, 2005, 42(9): 1057–1071.

[16] Yu Y, Zhong Q, Li C, *et al*. Identification and characterization of IL-1 receptor-associated kinase-4 (IRAK-4) in half-smooth tongue sole *Cynoglossus semilaevis* [J]. Fish & Shellfish Immunology, 2012, 32(4): 609–615.

[17] Liu Y, Yu S, Chai Y, *et al*. Lipopolysaccharide-induced gene expression of interleukin-1 receptor-associated kinase 4 and interleukin-1β in roughskin sculpin (*Trachidermus fasciatus*) [J]. Fish & Shellfish Immunology, 2012, 33(4): 690–698.

[18] Brietzke A, Goldammer T, Rebl H, *et al*. Characterization of the interleukin 1 receptor-associated kinase 4 (IRAK4)-encoding gene in salmonid fish: the functional copy is rearranged in *Oncorhynchus mykiss* and that factor can impair TLR signaling in mammalian cells [J]. Fish & Shellfish Immunology, 2014, 36(1): 206–214.

[19] Umasuthan N, Bathige S D, Whang I, *et al*. Insights into molecular profiles and genomic evolution of an IRAK4 homolog from rock bream (*Oplegnathus fasciatus*): immunogen- and pathogen-induced transcriptional expression [J]. Fish & Shellfish Immunology, 2015, 43(2): 436–448.

[20] 黄郁葱, 鲁义善, 简纪常, 等. 红笛鲷IRAK-4基因cDNA全长的克隆及组织表达分析[J]. 广东海洋大学学报, 2015, 35(1): 18–27.
Huang Y C, Lu Y S, Jian J C, *et al.* Full-length c DNA cloning and tissue expression analysis of IRAK-4 gene from humphead snapper(*Lutjanus sanguineus*) [J]. Journal of Zhanjiang Ocean University, 2015, 35(1): 18–27(in Chinese).

[21] Hu X Q, Fu X Z, Li N Q, *et al*. Transcriptomic analysis of mandarin fish brain cells infected with infectious spleen and kidney necrosis virus with an emphasis on

retinoic acid-inducible gene 1-like receptors and apoptosis pathways [J]. Fish & Shellfish Immunology, 2015, 45(2): 619–629.

[22] 吴明皇, 常藕琴, 石存斌, 等. 鳜鱼TCRα基因实时荧光定量RT-PCR检测方法的建立[J]. 广东农业科学, 2011, 38(6): 1–5.
Wu M H, Chang O Q, Shi C B, *et al*. Establishment of a real-time fluorescent quantitative RT-PCR assay for detection of *Siniperca chuatsi*'s TCRα gene [J]. Guangdong Agricultural Sciences, 2011, 38(6): 1–5(in Chinese).

[23] 时云朵, 任燕, 张德锋, 等. 山莨菪碱提高嗜水气单胞菌灭活疫苗浸泡免疫鲫的效果[J]. 水产学报, 2015, 39(5):720–727.
Shi Y D, Ren Y, Zhang D F, *et al*. Anisodamine increases efficacy of *Aeromonas hydrophila* inactivated vaccine in gibel carp *Carassius auratus gibelio* by immersion immunization [J]. Journal of Fishery of China, 2015, 39(5):720–727(in Chinese).

[24] Fu X Z, Li N Q, Lin Q, *et al*. Protective immunity against infectious spleen and kidney necrosis virus induced by immunization with DNA plasmid containing mcp gene in Chinese perch *Siniperca chuatsi*[J]. Fish & Shellfish Immunology, 2014, 40(1):259–266.

[25] Ye H, Arron J R, Lamothe B, *et al*. Distinct molecular mechanism for initiating TRAF6 signalling [J]. Nature, 2002, 418(6896): 443–447.

[26] Ohnishi H, Tochio H, Kato Z, *et al*. Structural basis for the multiple interactions of the MyD88 TIR domain in TLR4 signaling [J]. Proceedings of the Ntional Aademy of Siences of The United States of America, 2009, 106(25): 10260–10265.

[27] Bakkemo K R, Mikkelsen H, Bordevik M, *et al*. Intracellular localisation and innate immune responses following *Francisella noatunensis* infection of Atlantic cod (*Gadus morhua*) macrophages [J]. Fish & Shellfish Immunology, 2011, 31(6): 993–1004.

[28] Yamashita M, Yamashita Y, Ando T, *et al*. Identification and determination of selenoneine, 2-Selenyl-N-alpha, N-alpha, N-alpha-Trimethyl-L-Histidine, as the major organic selenium in blood cells in a fish-eating population on remote Japanese Islands [J]. Biological Trace Element Research, 2013, 156(1–3): 36–44.

[29] MEnke a L, Spitsbergen J M, Wolterbeek A P, *et al*. Normal anatomy and histology of the adult zebrafish [J]. Toxicologic Pathology, 2011, 39(5): 759–775.

[30] Uribe C, Folch H, Enriquez R, *et al*. Innate and adaptive immunity in teleost fish: a review [J]. Veterinarni Medicina, 2011, 56(10): 486–503.

[31] Ellis A E. Innate host defense mechanisms of fish against viruses and bacteria [J]. Development and Comparative Immunology, 2001, 25(8–9): 827–839.

[32] Möller A M, Korytář T, Köllner B, *et al*. The teleostean liver as an immunological organ: intrahepatic immune cells (IHICs) in healthy and benzo[a]pyrene challenged rainbow trout (*Oncorhynchus mykiss*) [J]. Development and Comparative Immunology, 2014, 46(2): 518–529.

[33] Raida M K, Buchmann K. Innate immune response in rainbow trout (*Oncorhynchus mykiss*) against primary and secondary infections with *Yersinia ruckeri* O1[J]. Developmental & Comparative Immunology, 2009, 33(1): 35–45.

[34] Roca F J, Sepulcre M P, López-Castejón G, *et al*. The colony-stimulating factor-1 receptor is a specific marker of macrophages from the bony fish gilthead seabream[J]. Molecular Immunology, 2006, 43(9): 1418–1423.

[35] Tsujita T, Tsukada H, Nakao M, *et al*. Sensing bacterial flagellin by membrane and soluble orthologs of Toll-like receptor 5 in rainbow trout (*Onchorhynchus mikiss*)[J]. Journal of Biological Chemistry, 2004, 279(47): 48588–48597.

[36] Chen W J, Guo C J, Zhou Z C, *et al*. Molecular cloning of IKKβ from the mandarin fish (*Siniperca chuatsi*) and its up-regulation in cells by ISKNV infection[J]. Veterinary Immunology and Immunopathology, 2011, 139(1): 61–66.

[37] Suzuki N, Suzuki S, Duncan G S, *et al*. Severe impairment of interleukin-1 and Toll-like receptor signalling in mice lacking IRAK-4 [J]. Nature, 2002, 416(6882): 750–756.

[38] Krug A, French A R, Barchet W, *et al*. TLR9-dependent recognition of MCMV by IPC and DC generates coordinated cytokine responses that activate antiviral NK cell function [J]. Immunity, 2004, 21(1): 107–119.

[39] Yang K, Puel A, Zhang S, *et al*. Human TLR-7-, -8-, and -9-mediated induction of IFN-alpha/beta and -lambda Is IRAK-4 dependent and redundant for protective immunity to viruses [J]. Immunity, 2005, 23(5): 465–478.

Cloning and expression profiling of Sc*IRAK*4 gene in mandarin fish (*Siniperca chuatsi*)in response to virus infections

LIN Qiang[1, 2], YANG Song[3], LI Ningqiu[1, 2 *], FANG Xiang[1],
FU Xiaozhe[1, 2], LIU Lihui[1, 2], GUO Huizhi[1, 2], LI Wangli[3], WU Shuqin[1, 2]

(1. *Key Laboratory of Aquatic Animal Immune Technology*, *Guangdong Province*, *Key Laboratory of Fishery Drug Development*, *Ministry of Agriculture*, *Pearl River Fisheries Research Institute*, *Chinese Academy of Fishery Sciences*, *Guangzhou* 510380, *China*;
2. *Freshwater Aquaculture Collaborative Innovation Center of Hubei Province*, *Wuhan* 430070, *China*;
3. *College of Animal Science and Technology*, *Sichuan Agricultural University*, *Chengdu* 611130, *China*)

Abstract: As a pivotal signaling mediator of Toll-like receptor (TLR) and interleukin (IL)-1 receptor (IL-1R) signaling cascades, the IL-1R-associated kinase 4 (*IRAK*4) is engaged in the activation of host immunity. To study its biological function in mandarin fish (*Siniperca chuatsi*), the expression profiling of the gene and its role in immune responses to the infection of infectious spleen and kidney necrosis virus (ISKNV) and S. chuatsi Rhabdovirus (SCRV) were investigated. Based on the unigene sequences of *IRKA4* gene which was obtained from the transcriptomic results of *S. chuatsi*, specific primers were designed and the complete *IRKA4* gene (named *ScIRAK*) was cloned and sequenced by SMART-RACE. Bioinformatics analysis demonstrated that the CDS of *ScIRAK*4 gene was 1389bp, encoding a 462 amino acid with an N-terminal death domain (DD) and a central protein kinase domain (PKc). The transcription profiles of *IRAK*4 in the tissues of *S. chuatsi* were characterized by fluorescent quantitative RT-PCR. The results showed that the highest mRNA expression was found in the liver (P<0.05), followed by that in the muscle, blood, brain and stomach (P<0.05). The transcriptions of the *IRAK*4 in the spleen of mandarin fish infected with ISKNV or SCRV were furtherly analyzed. The mRNA of *ScIRAK*4 was down-regulated in the mandarin fish infected with ISKNV and the lowest transcription was observed at 24 h post infection (P<0.01). By contrast, the mRNA of *ScIRAK*4 was up-regulated in the mandarin fish infected with SCRV and the higest transcription was observed at 12h post of the infection (P<0.01). These findings suggest that *ScIRAK*4 plays a crucial and different role in the immune responses of Mandarin fish infected with different viruses.

Key words: *Siniperca chuatsi*; *ScIRAK*4; gene cloning; expression profiling

Corresponding author: LI Ningqiu. E-mail: liningq@126.com

Funding projects: National Key Technology R&D Program (2012BAD25B02); National Natural Science Fund (31502201); Special Funds for the Science and Industry Development from the Administration of Ocean and Fisheries of Guangdong Province (A201501B12)